

Learning Scene Flow in 3D Point Clouds

Xingyu Liu* Charles R. Qi* Leonidas J. Guibas

Stanford University

Abstract. Many applications in robotics and human-computer interaction can benefit from an understanding of 3D motion of points in a dynamic environment, widely noted as scene flow. While most previous methods focus on solving the problem with stereo and RGB-D images, few try to estimate scene flow directly from point clouds. In this work, we propose a novel deep neural network named *FlowNet3D* that learns scene flow from point clouds in an end-to-end fashion. Our network simultaneously learns deep hierarchical point cloud features, flow embeddings as well as how to smooth the output. We evaluate the network on both challenging synthetic data and real LiDAR scans from KITTI. Trained on synthetic data only, our network is able to generalize well to real scans. Benefited from learning directly in point clouds, our model achieved significantly more accurate scene flow results compared with various baselines on stereo images and RGB-D images.

Keywords: motion, scene flow, point cloud, deep learning

1 Introduction

Scene flow is the three-dimensional motion field of points in the world [1]. It provides a low-level understanding of a dynamic environment, without any assumed knowledge of structure or motion of the scene. With this flexibility, scene flow has many applications in robot perception/manipulation (such as motion-based object segmentation and trajectory prediction) and human-computer interaction (such as action recognition in videos). Since scene flow is 3D in its nature, to estimate it we need more than monocular 2D images – either multiple 2D views (stereo images) or knowledge of structure (from depth sensors) is required. There are abundant works in both of these branches. [2,3,4,5] are representative ones that jointly estimate structure and motion from consecutive frames of stereo image pairs. [6,7,8,9,10] extend optical flow estimation in RGB images to RGB-D case by introducing new constraints and regularization terms from the depth channel.

Although current methods focus on stereo and depth images, there are several reasons 3D point cloud is a preferred representation for estimating scene flow. First, computing scene flow directly from 3D points frees us from distortions caused by the projective transform to image planes. Imagine two cars driving

* indicates equal contributions.

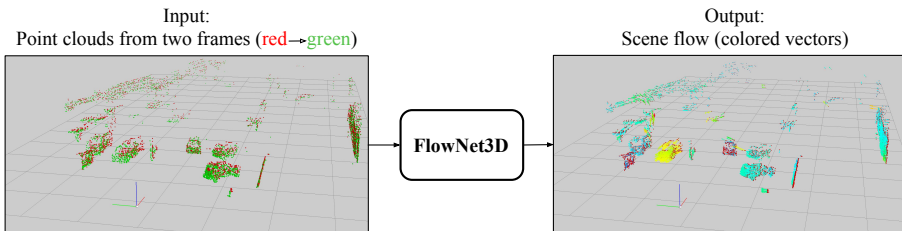


Fig. 1. End-to-end scene flow prediction from point clouds (best viewed in color). Our network directly consumes *raw point clouds* from two consecutive frames, and outputs dense scene flow for all points in the 1st frame. Above shows a LiDAR scan from KITTI, captured by a moving vehicle on road. Ground points are removed in a preprocessing step.

ahead of us, with one car in front of the other. While they are far away in depth, when projected to the image, the two cars become close to each other in pixels, resulting in strong occlusions and making it hard to estimate accurate scene flow along object boundaries. In contrast, point cloud based methods will not have to deal with such interference, since point clouds of these two cars are naturally separated in space. Second, working in point cloud format avoids assumptions of pixel or patch brightness constancy, a typical assumption in image based methods. Not relying on brightness constraints, point cloud based methods can be more robust in scenes with abrupt lighting changes such as sun flares and shadows in outdoor environments. With less reliance on color, we can also easily generalize the method to dark (night) environments and to objects or scenes with little texture. Finally, point clouds allow easier 3D transformations than images, and therefore could lead to easier formulation of the problem. One common case is when we know the camera motion (with visual odometry or SLAM) – we can then transform point clouds from all frames into a world coordinate systems so that points of static objects will stay static across frames. The problem thus becomes more controlled because most (background) points have zero motion. In contrast, image based methods still have to estimate relatively large motions for all pixels.

Despite all the advantages above, there has been little work studying scene flow estimation from point clouds. While [11] consider a similar problem to ours, they adopt hand-crafted point cloud features for an energy minimization formulation, and rely on a strong assumption that points in consecutive frames have correspondences, which is often not the case for partial scans (there will be missing and newly appearing points from frame to frame). Very recently, [12] introduces more learning in its pipeline but the approach is still restricted by manually designed features and simple logistic classifiers (for background filtering and correspondence classification).

In this work, inspired by the success of FlowNet [13], we take a deep learning approach for the problem. Our end-to-end learning solution can enable a deep

network to discover specialized features for scene flow and then seamlessly integrate feature extraction and flow prediction. Such an approach can also adapt to the particular data we have, and therefore avoid strong assumptions such as point correspondence or local rigidity. To design an end-to-end deep network for scene flow, we have to explore a large space of possible architectures. We have to at least answer three key questions: (1) how to learn point cloud features, (2) where in the network architecture to mix (to compare or associate) representations of point clouds from consecutive frames, and (3) how to mix them? In this work, we systematically explore the design space and present different choices and their trade-offs.

Based on the lessons learned in the design space exploration, we present a deep neural network called *FlowNet3D*, learning scene flow from point clouds in an end-to-end fashion. Our deep network simultaneously learns deep hierarchical features from point clouds and predicts an accurate 3D motion vector for each point. Instead of explicitly solving a correspondence problem, the network learns to collect and combine information necessary for a flow prediction. This is achieved by a novel *flow embedding* layer, which learns to aggregate information from geometric feature correlations as well as relative point displacements, by a shared neural network across space. In order to encourage smooth flow prediction, we propose a novel *set upconv* layer for point clouds. Compared to previous work that uses a non-parametric layer with 3D interpolation [14], our new layer has trainable parameters and is therefore more flexible and powerful. Through learned up-propagation of flow embeddings, we find the network is able to resolve ambiguous cases caused by symmetry, by integrating both local flow and global context. Notably, both the flow embedding layer and the set upconv layer can be realized through a shared learning module (Sec. 3.2) – thus our entire network is homogeneous, easy to parallelize and guaranteed to be permutation invariant to input point order.

We evaluate our model on both synthetic dataset and real LiDAR scans from KITTI. Our method shows competitive or better performance as compared to classic stereo and RGB-D image-based methods. Ablation studies further verify the effectiveness of our design choices and novel network layers. More remarkably, our deep net trained on synthetic data, without any modification, can robustly estimate scene flow in point clouds from real scans, showing its great generalizability.

In the following sections, we first review previous work in Section 2. In Section 3, we discuss the design space of deep networks for scene flow estimation and present our FlowNet3D architecture. Then in Section 4, we dwell more on our training process and a few techniques for better and layer parameters. In Section 5, we show both quantitative and qualitative results on FlyingThings3D and KITTI datasets. Finally, Section 6 concludes the paper.

2 Related Work

Scene flow from RGB or RGB-D images. Vedula et al. [1] first introduced the concept of scene flow, as three-dimensional field of motion vectors in the world. They assumed knowledge of stereo correspondences and combined optical flow and first-order approximations of depth maps to estimate scene flow. Since this seminal work, many others have tried to jointly estimate structure and motion from stereoscopic images [2,15,16,17,18,3,4,19,20,21,5], mostly in a variational setting with regularizations for smoothness of motion and structure [2,20,17], or with assumption of the rigidity of the local structures [19,5,21].

With the recent advent of commodity depth sensors, it has become feasible to estimate scene flow from monocular RGB-D images [6], by generalizing variational 2D flow algorithms to 3D [7,8] and exploiting more geometric cues provided by the depth channel [9,22,10]. Our work focuses on learning scene flow directly from *point clouds*, without any dependence on RGB images or assumptions on rigidity and camera motions.

Scene flow from point clouds. Scene flow is 3D motion of points in our world, and on the other hand point cloud is a natural representation of the 3D world. Therefore, it is both theoretically interesting and practically meaningful to study scene flow estimation directly from point clouds. However, this is a much under-explored area, and to the best of our knowledge, there has not been any deep learning based methods for this problem.

Very recently, Dewan et al. [11] proposed to estimate dense rigid motion fields in 3D LiDAR scans. They formulate the problem as a energy minimization problem of a factor graph, with hand-crafted 3D descriptors (SHOT [23]) for correspondence search among points between two frames and regularization terms to preserve motion smoothness. Later, Ushani et al. [12] present a different pipeline: they firstly convert point clouds to an occupancy grid, use a learned background filter to remove static voxels, and then train a logistic classifier to tell whether two columns of occupancy grids correspond. They then formulate a EM algorithm to estimate a locally rigid and non-deforming flow. Compared to these two previous work, our method is a cleaner and end-to-end solution with deep learned features and no dependency on hard correspondences or assumptions on rigidity.

Related deep learning based methods. While there is no previous work using deep learning that estimates scene flow from point clouds, there are a few using deep learning for optical flow and 3D local feature learning.

FlowNet [13] and FlowNet 2.0 [24] are two seminal works that propose to learn optical flow with convolutional neural networks in an end-to-end fashion, showing competitive performance with great efficiency. [25] extends FlowNet to simultaneously estimating disparity and optical flow. Our work is inspired by the success of those deep learning based attempts at optical flow prediction, and can be viewed as the 3D counterpart of them. However, the irregular structure in point clouds (no regular grids as in image) presents new challenges and opportunities for design of novel architectures, which is the focus of this work.

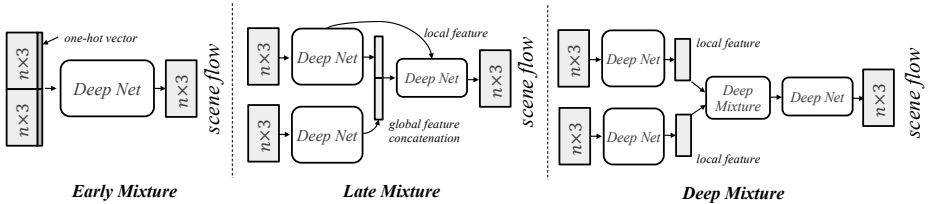


Fig. 2. Three meta-architectures for scene flow network. Inputs are two point clouds (n points with XYZ coordinates) from two frames, output is $n \times 3$ scene flow vector for each point in the first frame. Our FlowNet3D (Fig. 4) adopts the deep mixture scheme.

3 Network Architectures

In this section, we start by discussing design spaces of scene flow networks and showing three meta-architectures. Before diving into specific architectures, we review PointNet [26], a base learning module for point clouds. Finally, we present FlowNet3D, an instantiation of one of the meta-architectures, with deep flow mixture and two novel neural network layers.

3.1 Design Space of Networks for Scene Flow

As mentioned in the introduction section, to design an end-to-end deep network for scene flow, we have to at least answer three key questions:

- how to learn point cloud features?
- where in the network architecture to mix point representations from consecutive frames?
- how to mix them?

How to learn point cloud features? We follow the recently proposed PointNet++ architecture [14], a deep network that learns hierarchical point cloud features by recursively applying PointNets at local regions with increasing scales. Another alternative is to use global features as learned from PointNet [26] or EdgeConvNet [27], a choice that favors scenes with single objects but not ones with multiple objects moving independently.

Where to mix points from consecutive frames? To estimate relative motion between points, we have to let them interact, or get mixed. We think there are at least three meta-architectures: *early mixture*, *late mixture* and *deep mixture*, as shown in Fig. 2. An architecture with early mixture combines raw input point clouds before any feature learning. To note which frame a point comes from, one can add a one-hot vector (with length two) as an extra feature for each point. In contrast, late mixture only aggregates global features of the two point clouds. A processed global feature is further concatenated or propagated to each point

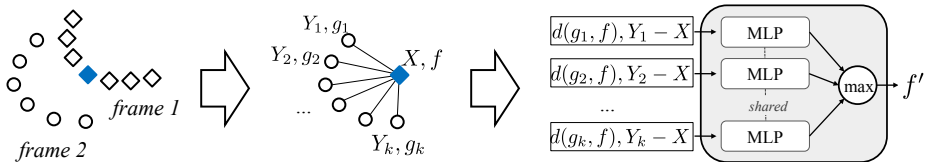


Fig. 3. Flow embedding layer. *Left:* We represent points in frame 1 as diamonds and those in the next frame as circles. For each of the points in frame 1, we want to compute its flow embedding. *Middle:* For a sample point (blue) in frame 1, with its 3D coordinate $X \in \mathbb{R}^3$ and local feature $f \in \mathbb{R}^c$, we find its neighboring points in frame 2 with coordinate Y_i and local features g_i , where $i = 1, 2, \dots, k$. *Right:* We use a base learning module, the gray block with multi-layer perceptrons (MLP) and max pooling, to aggregate distances of local point features and their displacements.

to predict its flow. Instead of mixing points at raw level or global feature level, we can also mix them at intermediate levels, mixing locally learned features of point clouds, a process we call deep mixture.

How to mix them? The simplest form of mixture is late mixture, global features from two point clouds are just concatenated and then further processed with fully connected layers. In both early mixture and deep mixture, we face two sets of point clouds (raw XYZ in early and local point feature plus XYZ for deep mixture). We will see in the next section that we can define a flow embedding layer that learns how to mix points for flow prediction. In experiments we will see that mixing points at the local feature level is much more effective than at the raw points level.

3.2 Review of PointNet [26]: A Base Learning Module for Point Clouds

Recently, seminal work by Qi et al. [26] proposed a novel neural network architecture for learning in point clouds. The architecture, named PointNet, in its simplest form, processes each point individually with a shared fully connected network across points, and then aggregate their outputs (point embeddings) through a max pooling function. Due to the symmetry of pooling, the network is guaranteed to be invariant to the ordering of the points.

Mathematically, the base learning module is defined as following. Given a point cloud of n orderless points: $\{x_1, x_2, \dots, x_n\}$ with $x_i \in \mathbb{R}^d$, our base learning module is a trainable set function $f : \mathcal{X} \rightarrow \mathbb{R}^c$

$$f(x_1, x_2, \dots, x_n) = \gamma \circ g(h(x_1), h(x_2), \dots, h(x_n)) \quad (1)$$

where, as in [26], we use multi-layer perceptron for h , element-wise max pooling for g , and fully connected layers for γ in further processing of the feature.

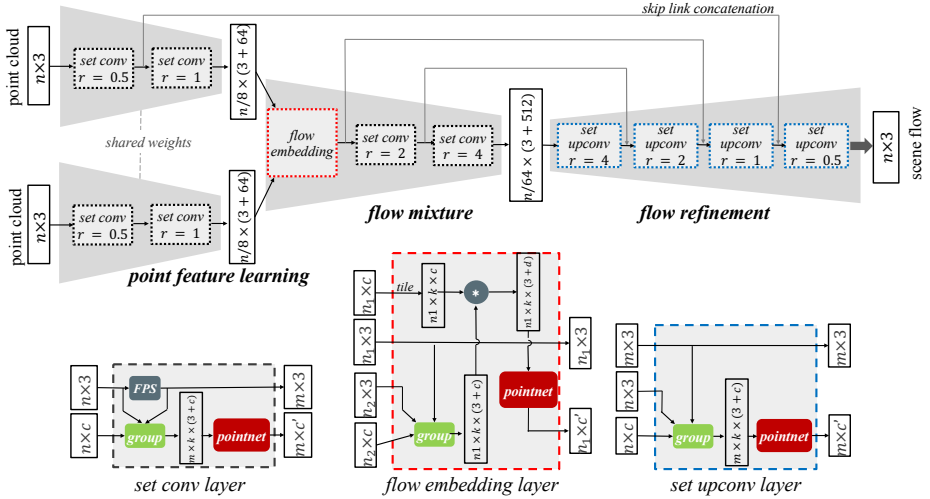


Fig. 4. FlowNet3D architecture. Given two frames of point clouds, the network learns to predict the scene flow as translational motion vectors for each point of the first frame. The r in layer blocks means radius, the range of point grouping. Below the network, we illustrate structures of three key layers used in the network. All these layers are built on the same base learning module (pointnet). Check Sec. 3.3 for description of the layers and Sec. 4 for more details on network parameters.

In this work, we extensively use this *pointnet*¹ module as a building block for our network, using it in many innovative ways specialized for scene flow estimation. See Fig. 3 Right (the gray block) and Fig. 4 for detailed use cases.

3.3 FlowNet3D: Learning Scene Flow in 3D Point Clouds

In this section, we explain the architecture of FlowNet3D and internal structures of its layers. Shown in Fig. 4, our proposed network follows the deep mixture meta-architecture and has three functional parts: (1) Point feature learning, (2) Flow mixture, and (3) Flow refinement. Within these parts are three key layers: set conv layer, flow embedding layer and set upconv layer. In the following sections, we provide a detailed introduction of the network and its layers.

Point feature learning with set conv layers. This part of the network learns local geometric features from raw point clouds (with XYZ coordinates). Since a point cloud is a *set* of points that is irregular and orderless, traditional convolutions do not fit. We therefore follow a recently proposed PointNet++ architecture [14], a translation-invariant network that learns hierarchical features.

¹ Lowercase to indicate it is not the original full network, but just a module.

Although it was designed for 3D classification and segmentation, we find its feature learning layers also powerful for the task of scene flow. Specifically, we will use its layer for set abstraction and call it *set conv layer* here.

Internal structure of the set conv layer is shown at Fig. 4 bottom left: Given n input points with XYZ ($n \times 3$) and optional local point features ($n \times c$), the layer firstly subsamples the n points to m points with a farthest point sampler (FPS). Then using these m points as centroids, a grouping process extracts k neighboring points around each of them (by either k-nn graph or radius search in 3D Euclidean space). Features of those points are directly grouped while their XYZ coordinates are translated to a local coordinate system (with the centroid at origin). The grouping leads to a batch of local points with size $m \times k \times (c+3)$, where $c+3$ means concatenated feature (c -dim) and XYZ (3-dim). A base learning module (pointnet) then consumes the batch and outputs a features vector for each of the m points ($m \times c'$), representing its updated local property.

Using the learned set conv layers, our network extracts local point features from each of the input point clouds independently while downsampling them to $n/8$ points. Those subsampled points from two frames, with their coordinates and local features, are then fed into the next part for their mixture.

Flow mixture with a flow embedding layer. Ideally, to find the scene flow for a point in frame 1, we want to find its corresponding point in frame 2 and then the flow is simply their relative displacement. However, in real data, there are often no correspondences between point clouds in two frames, due to viewpoint shift for example. It is still possible to estimate the scene flow though, because we can find multiple softly corresponding points in frame 2 and make a “weighted” decision. This is the general idea behind our flow embedding layer, a layer that learns to aggregate and process information from point pairs for scene flow prediction.

Fig. 3 shows how we compute a *flow embedding* that aggregates both feature distance and 3D displacements of local points, using the pointnet learning module: Given a distance function d between feature vectors, we pass each point pair’s feature distance $d(g_i, f)$ and spatial displacement $Y_i - X$ to a shared multi-layer perceptron, and then aggregate all point pairs with a element-wise max pooling function. The max function is playing a selection role, selecting the most informative signals from all point pairs. We call the outputs f' of this layer flow embeddings, as they implicitly encode information about the flow, a result of our end-to-end training of the network to predict scene flow:

$$f' = \text{MAX}_{i=1, \dots, k} \{h(d(g_i, f), Y_i - X)\} . \quad (2)$$

The distance function for the local point features includes Euclidean distance, cosine distance, element-wise L1/L2 distance (a distance for each dimension of the feature vector) etc. Beyond those, we can even let the network learn its own distance, by directly feeding both feature vectors from the point pair into the multi-layer perceptron. Empirically, we find this network-learned distance performs the best on the benchmark dataset.

Note that while Fig. 3 shows how we compute flow embedding for a single point in frame 1, Fig. 4 (bottom middle) provides a more complete structure of the flow embedding layer.

Although we can directly use the flow embedding with a simple following linear layer for flow prediction, there are two reasons against it. First, the current flow embedding still relies on very local features with small receptive fields, therefore it is hard to resolve ambiguous or symmetry cases. For example, for a translating flat plane, in local perspective, any local features are equally similar to each other, how can the network know its true moving direction? This becomes possible though, if let flows talk to each other by increasing its receptive fields through set conv and set upconv layers (as in flow mixture and flow refinement). Second, the flow embedding is computed on the intermediate feature level, where the point cloud is already down sampled. We need to “upsample” the flow embedding in order to predict flow for all the original points, a topic we discuss below.

Flow refinement with trainable set upconv layers. In this part of the network, we want to propagate flow embeddings from the subsampled points to all original points in frame 1. This is a similar task to what faced by the feature propagation stage described in [14], where features need to be upsampled for object part segmentation and scene semantic segmentation tasks. However, in the previous work [14], the feature propagation layer is not trainable. It is just a predefined 3D interpolation layer with inverse distance weights – it has no ability in learning how to up propagate flow embeddings.

In this work, we propose a novel trainable layer for feature up propagation – *set upconv layer* as shown in Fig. 4 (bottom right). It is very similar to set conv layer except that instead of having a farthest point sampler to subsample the points, a set upconv layer directly takes $m \times 3$ coordinates to indicate where we want to upsample to. Those $m \times 3$ coordinates are exactly those from the corresponding set conv layers in flow mixture or point feature learning parts.

Now compared to using 3D interpolation, our network learns how to weight the nearby points’ features, just as how the flow embedding layer weight displacements. We will show that the new set upconv layer shows significant advantage in empirical results.

4 Implementation Details

4.1 Architecture and Training Details

Every layer in FlowNet3D involves a base learning module, thus has a few fully connected layers as a multi-layer perceptron (MLP). Additional, a set conv or set upconv layer has a optional subsampling rate and a search radius (or a k for k-nn search). For the two set conv layers in the point feature learning part, we have set conv 1 with $mlp\{32, 32, 64\}$, $r = 0.5$ and subsample rate 2x, and set conv 2 with $mlp\{64, 64, 128\}$, $r = 1.0$ and subsample rate 4x. In the

flow mixture part, the flow embedding layer has $mlp\{128, 128, 128\}$ and searches for at most 64 k-nn points (in the other frame) within a radius of 5. The next two conv set layers have $mlp\{128, 128, 256\}$, $r = 2.0$, subsample rate 4x and $mlp\{256, 256, 512\}$, $r = 4.0$, subsample rate 4x, respectively. For the flow refinement part, we have four set up conv layers, they have corresponding radius to the set conv layers with $mlp\{128, 128, 256\}$, $mlp\{128, 128, 256\}$, $mlp\{128, 128, 128\}$ and $mlp\{128, 128, 128\}$ respectively. Finally, we have a linear layer that predicts a \mathbb{R}^3 scene flow from flow embedding of each of the points in frame 1.

We use smooth L1 loss for our scene flow regression. For optimization we use Adam optimizer with initial learning rate of 0.001. We use a step-wise decay schedule, reducing the learning rate by 30% every 20 epochs. We deploy batch normalizations for all layers except for the last fully connected one for flow prediction, and initialize the batch decay as 0.5 for a fast update and gradually decay the batch decay to 0.99. We use a batch size of 16 with randomly down sampled 2,048 points for each frame during training. The random sampling also augments the data.

4.2 Inference with FlowNet3D

Our network can support a variable number of input points, or even different number of points between the two frames, without the necessity to retrain the network. This is possible because we repetitively use the same base learning module across the entire network (for set conv, flow embedding and set upconv), which is agnostic to the number of input points.

Another special challenge with regression problems (such as scene flow) in point clouds is that down-sampling introduces noise in prediction. A simple but effective way to reduce the noise is to randomly re-sample the point clouds for multiple inference runs and average the predicted flow vectors for each point. In the experiments, we will see that this re-sampling and averaging step leads to a slight performance gain.

5 Experiment Results

In this section, we evaluate performance of FlowNet3D, verify our design choices with ablation studies, and finally provide visualizations to understand what the network has learned.

5.1 Evaluation and Design Validation on FlyingThings3D

Training deep neural networks for scene flow estimation requires labeled training data. To the best of our knowledge, FlyingThings3D [25] is the only existing dataset with point clouds (depth) and ground truth scene flow, and at the same time exceeds a size of 10k samples. The dataset consists of rendered scenes with multiple randomly moving objects sampled from ShapeNet [31], a large repository of 3D shapes. There are in total around 32k stereo images with

Table 1. Flow estimation results on FlyingThings3D dataset. Metrics are End-point-error (EPE) 2D and Acc 2D (<3px or 5%) for (projected) optical flow; and EPE 3D, Acc 3D (<0.05 or 5%, <0.1 or 10%) for 3D scene flow.

Method	Input	EPE 2D	EPE 3D	Acc2D	Acc3D (0.05)	Acc3D (0.1)
Classic+NLP [28]	RGB	37.80	-	12.14%	-	-
LDOF [29] + depth	RGBD	29.42	-	17.63%	-	-
ICP [30]	points	31.73	0.5019	18.48%	7.62%	21.98%
Early-Mixture (ours)	points	33.11	0.5807	7.72%	2.64%	12.21%
Late-Mixture (ours)	points	45.08	0.7876	2.06%	0.27%	1.83%
Deep-Mixture (ours)	points	20.82	0.3401	15.31%	4.87%	21.01%
FlowNet3D (ours)	points	10.71	0.1694	39.95%	25.37%	57.85%

Table 2. Ablation studies on FlyingThings3D dataset. We study the effects of distance function, type of pooling in pointnet module, layers used in flow refinement and average voting by resampling.

Distance func.	Pooling	Refine	Resample	EPE 2D	EPE 3D
dot product	avg	interp	N	18.86	0.3163
dot product	max	interp	N	14.88	0.2463
cosine	max	interp	N	15.65	0.2600
learned	max	interp	N	13.92	0.2298
learned	max	upconv	N	11.50	0.1835
learned	max	upconv	Y	10.71	0.1694

ground truth disparity and optical flow maps. We randomly subsampled 20,000 of them as our training set and 2,000 as our test set. Instead of using RGB images, we preprocess the data by popping up disparity maps to 3D point clouds and optical flow to scene flow.

Table 1 reports flow evaluation results on our FlyingThings3D test set. We evaluate with both 2D and 3D metrics. EPE 2D is end-point-error for projected scene flow (i.e. optical flow) and Acc 2D is the ratio of optical flow predictions that are less than 3 pixels or 5% relative off from the ground truth flow. EPE 3D and Acc 3D are counter parts defined in 3D space for scene flow. We have two Acc 3D metrics, a strict one and another more relaxed one. Among the baselines: Classic+NLP optimizes optical flow with Markov random field. It does not use depth information thus fails to capture 3D motion cues. LDOF+depth uses a variational model to solve optical flow and treats depth as an extra feature dimension – in that way the method does not fully exploit 3D geometry. The ICP (iterative-closest point) method, while simple and effective for single objects or static scenes, has a hard time to estimate motions for dynamic ones.

We also report three baseline deep networks in each of the meta-architectures (Fig. 2). They all share similar parameters for set conv and feature propagation layers [14]. Among them, Early-Mixture baseline (4th row in table) combines point clouds at the raw points level, by appending points with a length-two one-hot feature vector indicating which frame (1 or 2) they belong to. However, unlike

Table 3. Optical flow and scene flow results on KITTI scene flow dataset (train set). Metrics are 2D end-point-error (EPE) and 2D outlier ratio (>3px or 5%) for optical flow, and 3D EPE, 3D outlier ratio (>0.3m or 5%) for 3D scene flow. KITTI ranking is method’s ranking on KITTI scene flow leaderboard. Our FlowNet3D model is trained on the synthetic FlyingThings3D dataset.

Method	Input	2D EPE (pixels)	2D outliers (3px or 5%)	3D EPE (meters)	3D outliers (0.3m or 5%)	KITTI ranking
LDOF [29]	RGB-D	9.79	35.03%	0.498	12.61%	21
OSF [32]	RGB-D	6.05	12.82%	0.394	8.25%	9
PRSM [33]	RGB-D	4.41	11.90%	0.327	6.06%	3
	RGB stereo			0.729	6.40%	
ICP (global)	points	17.61	68.90%	0.385	42.38%	-
ICP (segmentation)	points	10.56	17.39%	0.215	13.38%	-
FlowNet3D (ours)	points	5.82	46.40%	0.122	5.61%	-

images that have a good alignment of pixels, point clouds’ irregular structure makes their mixture much harder, leading to unsatisfactory results. Late-Mixture baseline (5th row in table) also performs poorly because point clouds vary greatly in their spatial regions and ranges from frame to frame, thus making it hard to efficiently encode flow information into a global feature vector. In contrast, the Deep-Mixture baseline (second last row in table) performs much better by mixing points at intermediate feature levels. Compared to FlowNet3D on how to mix points, the baseline method does not use a flow embedding layer, but rather takes a similar approach to FlowNet [13] in images. The Deep-Mixture baseline concatenates all feature distances and XYZ displacements into a long vector and passes it to a fully connected network before more set conv layers. This however results in suboptimal learning because it is highly affected by the point orders. Besides, compared to FlowNet3D, the baseline just uses 3D interpolation (with skip links) for flow refinement. See appendix for more details about architectures of our baseline models.

Table 2 shows the effects of several design choices on the performance of FlowNet3D. Comparing the first two rows, we see max pooling has a significant advantage over average pooling, probably because max pooling is more selective in picking “corresponding” point and suffers less from noise. Comparing row 2 to row 4, we see the effect of distance functions for our flow embedding layer. Interestingly, we find that letting the network learn its distance function (by inputting both of the feature vectors to the MLP) results in the best performance. If we look at row 4 and row 5, we will see that our newly proposed set upconv layer significantly reduces flow error. And lastly, during test time we find it helpful to average flow prediction by multiple runs with random subsampling (in set conv layers). We used 10 runs for the number reported in the last row.

5.2 Generalization to Real LiDAR Scans in KITTI

In this section, we show that our model, trained on the synthetic FlyingThings3D dataset, can be directly applied to detect scene flow in point clouds from

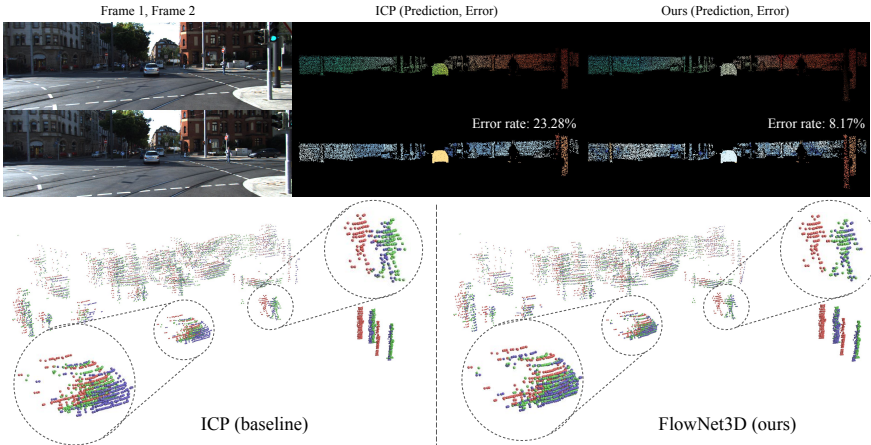


Fig. 5. Scene flow on KITTI point clouds. We show scene flow results on two examples with a ICP baseline (global) and our method. For each example, we visualize RGB images of consecutive frames (unused), scene flow projected to image plane (optical flow) and its error map compared to ground truth optical flow. Optical flow error rates are shown within each error map. We also show points from **frame 1**, **frame 2** and **estimated flowed points** in different colors.

KITTI scene flow dataset [34]. Given a LiDAR scan, we firstly preprocess the point clouds to remove its ground, as ground is a large piece of flat geometry that provides little cue to its motion but at the same time occupies a large portion of points, biasing the evaluation results². We then directly consume the raw point clouds with XYZ coordinates for scene flow prediction.

In Table 3, we provide quantitative results on optical flow and scene flow estimation on the KITTI scene flow dataset. Since no point cloud is provided for the test set (and part of the train set), we evaluate on all 150 out of 200 frames from the train set with available point clouds. We compare with prior arts optimized for 2D optical flow as well as two ICP baselines on point clouds. Among the baselines: LDOF is the same method we used in FlyingThings3D comparison. OSF uses discrete-continuous CRF on superpixels with the assumption of rigid motion of objects. PRSM uses energy minimization on rigidly moving segments and jointly estimates multiple attributes together including rigid motion. These three image based methods do not output scene flow directly (but optical flow and disparity separately), we either use estimated disparity (fourth row) or pixel depth change (first three rows) to compute depth-wise flow displacements. ICP (global) estimates a single rigid motion for the entire scene. ICP (segmentation) is a stronger baseline that first computes connected components on LiDAR

² Please see appendix on how we remove ground and more evaluation results on full point clouds without ground removal.

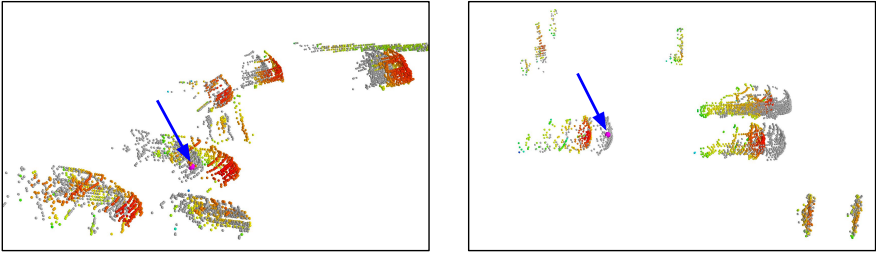


Fig. 6. Visualization of local point feature similarity. Given a point P (pointed by the blue arrow) in frame 1 (gray), we compute a heatmap indicating how points in frame 2 are similar to P in feature space. More red is more similar.

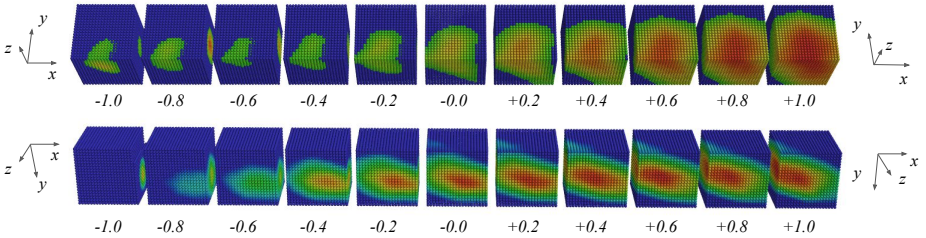


Fig. 7. Visualization of flow embedding layer. Given a certain similarity score (defined by one minus cosine distance), which of (x, y, z) displacement vectors in a $[-5, 5] \times [-5, 5] \times [-5, 5]$ cube can activate one output neuron of the flow embedding layer.

points after ground removal and then estimates rigid motions for each individual segment of point clouds.

While 2D methods [29,32,33] lead in optical flow estimation, our method shows great advantages on scene flow estimation – achieving significantly lower 3D end-point error (*63% relative error reduction* from [33]) and 3D outlier ratios. Our method also outperforms the two ICP baselines that rely more on rigidity of global scene or correctness of segmentation. Additionally, we can conclude that our model, although only trained on synthetic data, remarkably generalizes well to the real LiDAR point clouds.

Fig. 5 visualizes our scene flow prediction in both projected view and 3D point clouds, compared with the global ICP baseline. The ICP baseline registers the global point clouds by a single rigid motion, therefore fails in estimating flow for dynamic objects. In contrast, our model can accurately estimate flows for dynamic objects, such as moving vehicles and pedestrians.

5.3 Network Visualizations

Fig. 6 visualizes the local point features our network has learned, by showing a heatmap of correlations between a chosen point in frame 1 and all points in

frame 2. We can clearly see that the network has learned geometric similarity and is robust to partiality of the scan.

Fig. 7 shows what has been learned in a flow embedding layer. Looking at one dimension in the flow embedding layer, we are curious to know how feature distance (or similarity) and point displacement affect its activation value. To simplify the study, we use a model trained with cosine distance function (for feature distance) instead of network learned distance. We iterate distance values and displacement vector, and in Fig. 7 we see that as similarity grows from -1 to 1, the activation becomes significantly larger. We can also see that this dimension is probably responsible for a flow around positive Z direction.

6 Conclusion

In this paper, we have presented a novel deep neural network architecture that estimates scene flow directly from 3D point clouds. We have proposed a novel *flow embedding* layer that learns to aggregate feature similarity and point displacements for scene flow prediction, as well as a new *set upconv* layer. On both challenging synthetic dataset and real LiDAR point clouds, we have showed the superiority of our method over various baselines. We have also provided visualization to help understand the characteristics of learned point cloud features and the proposed flow embedding layer.

References

1. Vedula, S., Baker, S., Rander, P., Collins, R., Kanade, T.: Three-dimensional scene flow. In: Computer Vision, 1999. The Proceedings of the Seventh IEEE International Conference on. Volume 2., IEEE (1999) 722–729
2. Huguet, F., Devernay, F.: A variational method for scene flow estimation from stereo sequences. In: Computer Vision, 2007. ICCV 2007. IEEE 11th International Conference on, IEEE (2007) 1–7
3. Wedel, A., Brox, T., Vaudrey, T., Rabe, C., Franke, U., Cremers, D.: Stereoscopic scene flow computation for 3d motion understanding. International Journal of Computer Vision **95**(1) (2011) 29–51
4. Vogel, C., Schindler, K., Roth, S.: 3d scene flow estimation with a rigid motion prior. In: Computer Vision (ICCV), 2011 IEEE International Conference on, IEEE (2011) 1291–1298
5. Menze, M., Geiger, A.: Object scene flow for autonomous vehicles. In: Conference on Computer Vision and Pattern Recognition (CVPR). (2015)
6. Hadfield, S., Bowden, R.: Kinecting the dots: Particle based scene flow from depth sensors. In: 2011 International Conference on Computer Vision (ICCV). (Nov 2011) 2290–2295
7. Herbst, E., Ren, X., Fox, D.: Rgb-d flow: Dense 3-d motion estimation using color and depth. In: Robotics and Automation (ICRA), 2013 IEEE International Conference on, IEEE (2013) 2276–2282
8. Jaimez, M., Souiai, M., Gonzalez-Jimenez, J., Cremers, D.: A primal-dual framework for real-time dense rgb-d scene flow. In: Robotics and Automation (ICRA), 2015 IEEE International Conference on, IEEE (2015) 98–104

9. Quiroga, J., Brox, T., Devernay, F., Crowley, J.: Dense semi-rigid scene flow estimation from rgbd images. In Fleet, D., Pajdla, T., Schiele, B., Tuytelaars, T., eds.: *Computer Vision – (ECCV) 2014*, Cham, Springer International Publishing (2014) 567–582
10. Sun, D., Sudderth, E.B., Pfister, H.: Layered rgbd scene flow estimation. In: *2015 IEEE Conference on Computer Vision and Pattern Recognition (CVPR)*. (June 2015) 548–556
11. Dewan, A., Caselitz, T., Tipaldi, G.D., Burgard, W.: Rigid scene flow for 3d lidar scans. In: *Intelligent Robots and Systems (IROS), 2016 IEEE/RSJ International Conference on, IEEE (2016)* 1765–1770
12. Ushani, A.K., Wolcott, R.W., Walls, J.M., Eustice, R.M.: A learning approach for real-time temporal scene flow estimation from lidar data. In: *Robotics and Automation (ICRA), 2017 IEEE International Conference on, IEEE (2017)* 5666–5673
13. Dosovitskiy, A., Fischery, P., Ilg, E., Hazirbas, C., Golkov, V., van der Smagt, P., Cremers, D., Brox, T., et al.: Flownet: Learning optical flow with convolutional networks. In: *2015 IEEE International Conference on Computer Vision (ICCV), IEEE (2015)* 2758–2766
14. Qi, C.R., Yi, L., Su, H., Guibas, L.J.: Pointnet++: Deep hierarchical feature learning on point sets in a metric space. *arXiv preprint arXiv:1706.02413* (2017)
15. Pons, J.P., Keriven, R., Faugeras, O.: Multi-view stereo reconstruction and scene flow estimation with a global image-based matching score. *International Journal of Computer Vision* **72**(2) (2007) 179–193
16. Wedel, A., Rabe, C., Vaudrey, T., Brox, T., Franke, U., Cremers, D.: Efficient dense scene flow from sparse or dense stereo data. In: *European conference on computer vision, Springer (2008)* 739–751
17. Valgaerts, L., Bruhn, A., Zimmer, H., Weickert, J., Stoll, C., Theobalt, C.: Joint estimation of motion, structure and geometry from stereo sequences. In: *European Conference on Computer Vision, Springer (2010)* 568–581
18. Čech, J., Sanchez-Riera, J., Horaud, R.: Scene flow estimation by growing correspondence seeds. In: *Computer Vision and Pattern Recognition (CVPR), 2011 IEEE Conference on, IEEE (2011)* 3129–3136
19. Vogel, C., Schindler, K., Roth, S.: Piecewise rigid scene flow. In: *Computer Vision (ICCV), 2013 IEEE International Conference on, IEEE (2013)* 1377–1384
20. Basha, T., Moses, Y., Kiryati, N.: Multi-view scene flow estimation: A view centered variational approach. *International journal of computer vision* **101**(1) (2013) 6–21
21. Vogel, C., Schindler, K., Roth, S.: 3d scene flow estimation with a piecewise rigid scene model. *International Journal of Computer Vision* **115**(1) (2015) 1–28
22. Hornacek, M., Fitzgibbon, A., Rother, C.: Spheroflow: 6 dof scene flow from rgb-d pairs. In: *Proceedings of the IEEE Conference on Computer Vision and Pattern Recognition*. (2014) 3526–3533
23. Tombari, F., Salti, S., Di Stefano, L.: Unique signatures of histograms for local surface description. In: *European conference on computer vision, Springer (2010)* 356–369
24. Ilg, E., Mayer, N., Saikia, T., Keuper, M., Dosovitskiy, A., Brox, T.: Flownet 2.0: Evolution of optical flow estimation with deep networks. In: *IEEE Conference on Computer Vision and Pattern Recognition (CVPR)*. Volume 2. (2017)
25. Mayer, N., Ilg, E., Husser, P., Fischer, P., Cremers, D., Dosovitskiy, A., Brox, T.: A large dataset to train convolutional networks for disparity, optical flow, and

- scene flow estimation. In: 2016 IEEE Conference on Computer Vision and Pattern Recognition (CVPR). (June 2016) 4040–4048
26. Qi, C.R., Su, H., Mo, K., Guibas, L.J.: Pointnet: Deep learning on point sets for 3d classification and segmentation. *Proc. Computer Vision and Pattern Recognition (CVPR)*, IEEE (2017)
 27. Wang, Y., Sun, Y., Liu, Z., Sarma, S.E., Bronstein, M.M., Solomon, J.M.: Dynamic graph cnn for learning on point clouds. *arXiv preprint arXiv:1801.07829* (2018)
 28. Sun, D., Roth, S., Black, M.J.: A quantitative analysis of current practices in optical flow estimation and the principles behind them. *International Journal of Computer Vision (IJCV)* **106**(2) (Jan 2014) 115–137
 29. Brox, T., Malik, J.: Large displacement optical flow: Descriptor matching in variational motion estimation. *IEEE Transactions on Pattern Analysis and Machine Intelligence* **33**(3) (March 2011) 500–513
 30. Besl, P.J., McKay, N.D.: A method for registration of 3-d shapes. *IEEE Transactions on Pattern Analysis and Machine Intelligence (TPAMI)* **14**(2) (Feb 1992) 239–256
 31. Chang, A.X., Funkhouser, T., Guibas, L., Hanrahan, P., Huang, Q., Li, Z., Savarese, S., Savva, M., Song, S., Su, H., Xiao, J., Yi, L., Yu, F.: ShapeNet: An Information-Rich 3D Model Repository. Technical Report arXiv:1512.03012 [cs.GR], Stanford University — Princeton University — Toyota Technological Institute at Chicago (2015)
 32. Menze, M., Geiger, A.: Object scene flow for autonomous vehicles. In: CVPR 2015
 33. Vogel, C., Schindler, K., Roth, S.: 3d scene flow estimation with a piecewise rigid scene model. *IJCV* (2015) 1–28
 34. Menze, M., Heipke, C., Geiger, A.: Joint 3d estimation of vehicles and scene flow. In: ISPRS Workshop on Image Sequence Analysis (ISA). (2015)
 35. Abadi, M., Barham, P., Chen, J., Chen, Z., Davis, A., Dean, J., Devin, M., Ghemawat, S., Irving, G., Isard, M., et al.: Tensorflow: A system for large-scale machine learning. In: OSDI. Volume 16. (2016) 265–283

Appendix

A. Overview

In this supplementary, we provide more details for network architecture, show time and space complexity of our FlowNet3D model, and finally present more results visualization for KITTI [5] and FlyingThings3D [25] dataset.

B. More Architecture Details

In Fig. 8 and Fig. 9, we illustrate our baseline architectures for early mixture and late mixture, respectively. The early mixture model takes combined point clouds from two frames, with a length-two one-hot vector for each point to indicate whether it is from point cloud 1 or point cloud 2. For each *set conv* layer, the r means radius for local neighborhood search, the *mlp* means multi-layer perceptron used for the pointnet module of the layer, “sample rate” means how much we downsample the point cloud (for example 1/2 means we keep half of the original points). The *feature propagation* layer is originally defined in [14], where features from subsampled points are propagated to upsampled points by 3D interpolation (with inverse distance weights). Specifically, the for an upsampled point is interpolated by three k-nn points in the subsampled points. After this step, the interpolated features are then concatenated with the local features linked from the outputs of the set conv layers. Then for each point, its concatenated feature passes through a few fully connected layers, the widths of which are defined by $mlp\{l_1, l_2, \dots\}$ in the block.

The late mixture model in Fig. 9 firstly computes global feature from each of the two point clouds, then it concatenates the global features and further processes it with a few fully connected layers (mixture happens at global feature level), and finally concatenate the tiled global feature with local point feature from point cloud 1 to predict the scene flow.

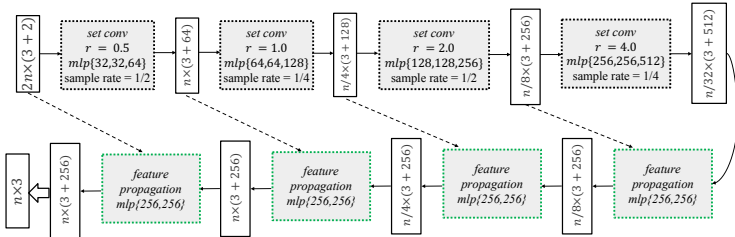


Fig. 8. Early Mixture Baseline Model.

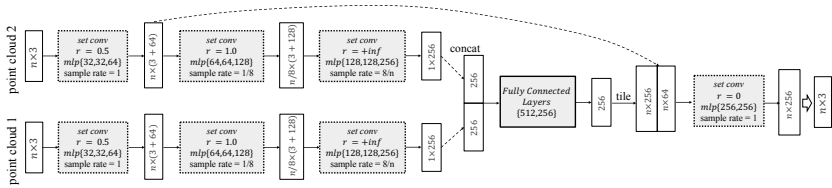


Fig. 9. Late Mixture Baseline Model.

C. Model Size and Runtime

FlowNet3D has a model size of 15MB, which is much more smaller than most deep convolutional neural networks. In Table 4, we show the inference speed of the model on point clouds with different scales. For this evaluation we assume both point clouds from the two frames have the same number of points as specified by #points. We test the runtime on a single NVIDIA 1080 GPU with TensorFlow [35] version 1.4 under Ubuntu 14.04. We can see that our model is able to run inference at with real-time capability.

Table 4. Runtime of FlowNet3D.

#points	1024	1024	2048	2048	4096	4096	8192
batch size	1	8	1	4	1	2	1
Time (ms)	18.5	43.7	36.6	58.8	101.7	117.7	325.9

D. Ground Removal

Ground is a large flat geometry with little feature to infer its motion, and it usually contains lots of points. With ground planes removed, scene flow results are less biased. It is also common to remove grounds in other LiDAR based methods [11,12]. In Table 5, we show how ground points affect scene flow results by evaluating on full point clouds. All methods in comparison are negatively impacted. But our method still outperforms the ICP baseline. By adopting ICP estimated flow on the segmented grounds and net estimated flow for the rest of points (last column in table), our method can also beat the prior art (PRSM).

Table 5. Scene flow results on KITTI (full point clouds).

Method	PRSM [33] (RGB-D)	ICP (global)	FlowNet3D (ours)	FlowNet3D + ICP
3D EPE	0.369	0.273	0.202	0.179
3D outliers	15.09%	27.92%	17.91%	13.57%

Table 6. Evaluation for ground segmentation. Accuracy is averaged across test frames.

Method	RANSAC	GroundSegNet
Accuracy	94.02%	97.60%
Time per frame	43 ms	57 ms

To validate we can effectively remove grounds in LiDAR point clouds, we evaluate two ground segmentation algorithms: RANSAC and GroundSegNet. RANSAC fits a tilted plane to point clouds and classify points close to the plane as ground points. GroundSegNet is a PointNet segmentation network trained to classify points (in 3D patches) to ground or non-ground (we annotated ground points in all 150 frames and use 100 frames as train and the rest as test set). Both methods can run in real time: 43ms and 57ms per frame respectively, and achieve very high accuracy: *94.02%* and *97.60%* averaged across test set. Note that for evaluation in Table 3, we use our annotated ground points for ground removal, to avoid dependency on the specific ground removal algorithm.

E. More Visualization for KITTI Results

In the main paper, we show quantitative evaluation and visualization for two sample frames from KITTI scene flow [5] dataset. Here we provide more details and show more examples.

The frame pairs used in the paper are 000149_10/000149_11 and 000119_10/000119_11 in KITTI scene flow dataset. The color coding of the flow follows the default coding used in the toolkit of KITTI scene flow dataset.

In the rest of this section, We show more scene flow results on two examples with a ICP baseline and our method. For each example, we visualize RGB images of consecutive frames (unused in point cloud experiments), scene flow projected to image plane (optical flow) and its error map compared to ground truth optical flow. Optical flow error rates are shown within each error map. We also show points from **frame 1**, **frame 2** and **estimated flowed points** in different colors. Ideal prediction would roughly align blue and green points. The results are illustrated in Figure 10-11.

F. Visualization for FlyingThings3D Results

We provide results and visualization of our method on FlyingThings3D test set [25]. The dataset consists of rendered scenes with multiple randomly moving objects sampled from ShapeNet [31]. To clearly visualize the complex scenes, we provide the view of the whole scene from top. We also zoom in and view each object from one or more directions. The directions can be inferred from consistent *xyz* coordinates shown in both the images and point cloud scene. We show points from **frame 1**, **frame 2** and **estimated flowed points** in different colors. Note that local regions are zoomed in and rotated for clear viewing. To help find

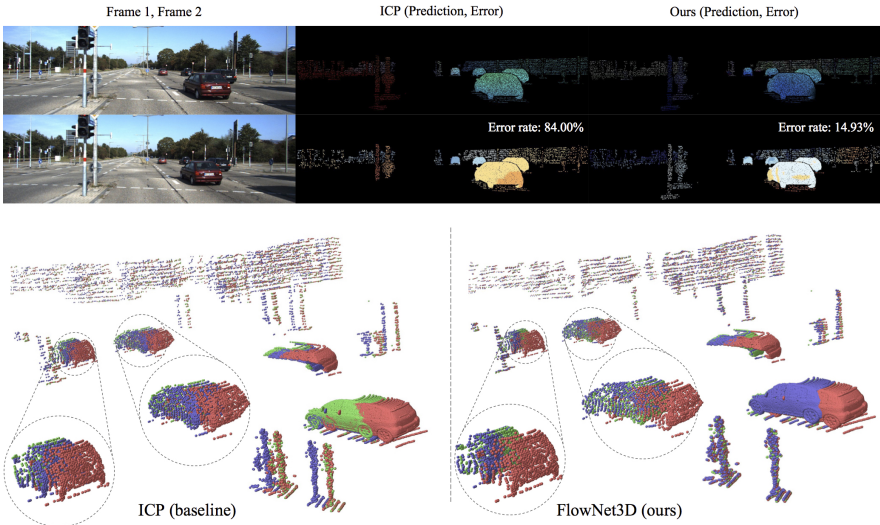


Fig. 10. Scene flow results for 000048_10/000048_11 pair of KITTI

correspondence between images and point clouds, we used distinct colors for zoom-in boxes of corresponding objects. Ideal prediction would roughly align blue and green points. The results are illustrated in Figure 12-14.

Our method can handle challenging cases well. For example, in the orange zoom-in box of Figure 12, the gray box is occluded by the sword in both frames and our network can still estimate the motion of both the sword and visible part of the gray box well. There are also failure cases, mainly due to the change of visibility across frames. For example, in the orange zoom-in box of Figure 14, the majority of the wheel is visible in the first frame but not visible in the second frame. Thus our network is confused and the estimation of the motion for the non-visible part is not accurate.

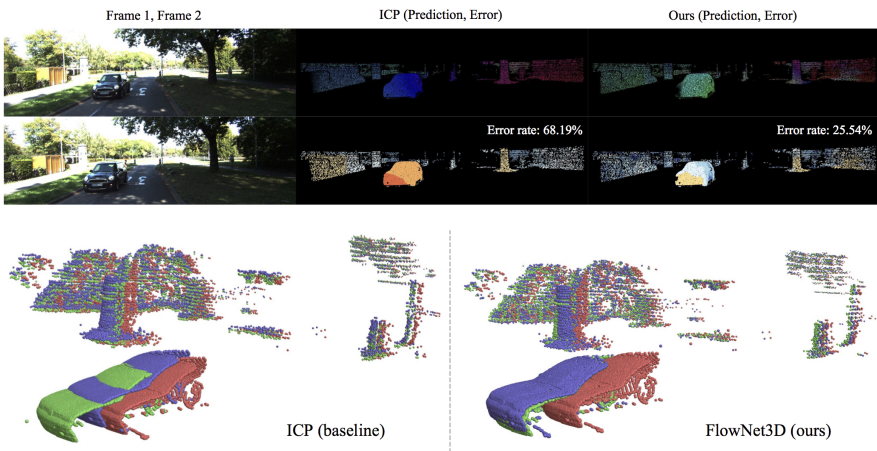


Fig. 11. Scene flow results for 000059_10/000059_11 pair of KITTI

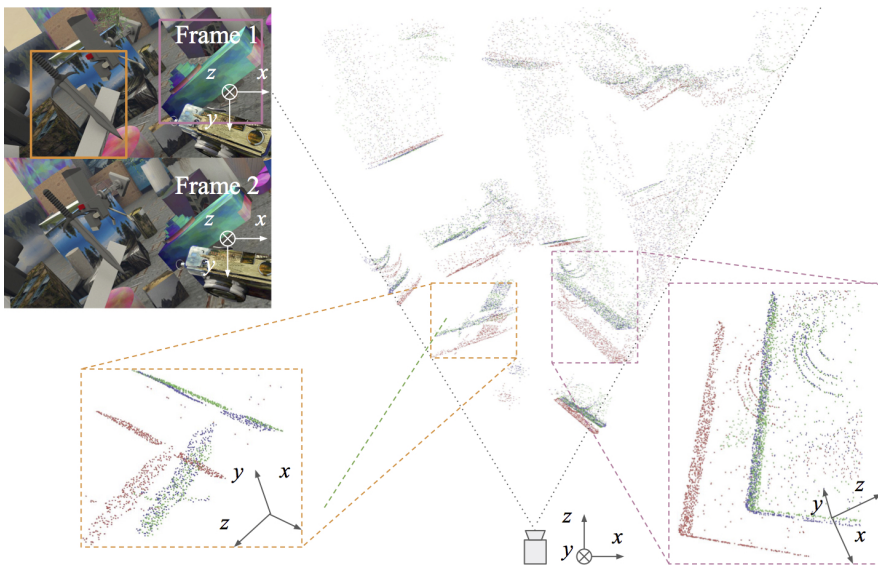


Fig. 12. Scene flow results for TEST-A-0061-right-0013 of FlyingThings3D.

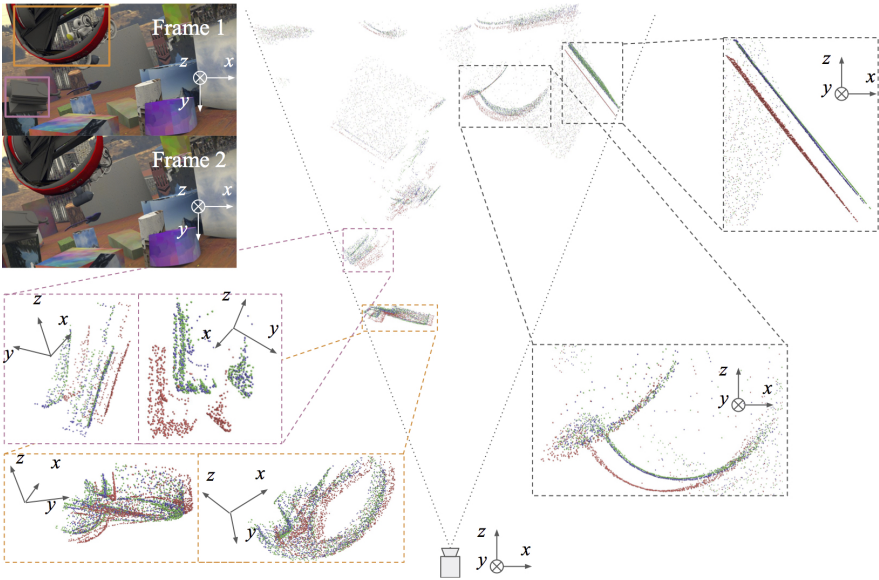


Fig. 13. Scene flow results for TEST-A-0006-right-0011 of FlyingThings3D.

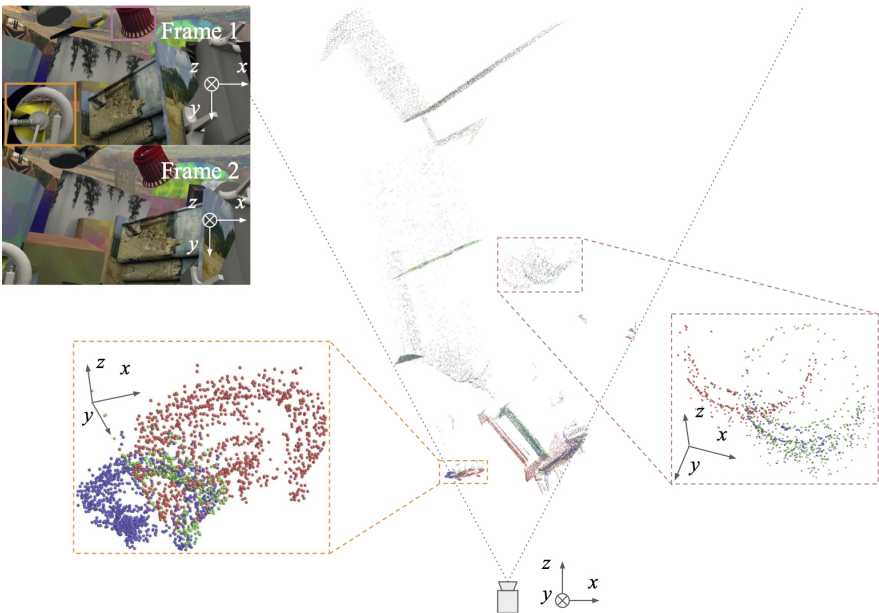


Fig. 14. Scene flow results for TEST-B-0011-left-0011 of FlyingThings3D.